

ENERGY DISPERSIVE X-RAY DIFFRACTION POTENTIALITY IN THE FIELD OF CULTURAL HERITAGE: SIMULTANEOUS STRUCTURAL AND ELEMENTAL ANALYSIS OF VARIOUS ARTEFACTS.

Eugenio CAPONETTI^(c),¹, Ruggero CAMINITI², Delia CHILLURA MARTINO¹, Maria Luisa SALADINO¹

1. Università degli Studi di Palermo, Dipartimento di Chimica Fisica "F. Accascina", Viale delle Scienze, P.co D'Orleans II - Pad. 17, I-90128 Palermo, Italy
2. Università degli Studi di Roma "La Sapienza", Dipartimento di Chimica, P.le A. Moro 5, I-00185 Roma, Italy

Summary. - The applicability of an Energy Dispersive X-ray Diffractometer to some technical questions in the field of Cultural Heritage is presented. This diffractometer, equipped with a white source, has been utilized for the structural and elemental analysis of some items having different nature. Given its design, the instrument allows to collect data from samples as big as a book or a little more. Samples, without collection of any portion and without any preliminary preparation, have been placed in the instrument and spectra have been collected in a wide energy range that contains X-ray fluorescence and diffraction features. In all cases, data acquired in air and in a non destructive way were reliable and their collection was fast. Fluorescence and X-ray diffraction information, when possible, have been compared with those obtained by XRF micro-analysis and by an Angle Dispersive X-ray Diffractometer equipped with a Cu X-ray source. By using the last two techniques, data have been collected from small areas of the samples.

INTRODUCTION

It is well known that X-rays allow the determination of both elemental composition and structure of a sample. Usually, commercial devices are designed to perform fluorescence or diffraction measurements. Recently, an Energy Dispersive X-ray Diffractometer (EDXD) has been built on Patent no. 01261484,1993 of "La Sapienza" University¹. It revealed to be well suited in order to perform measurements on liquid or solid samples and to achieve structural information of crystalline as well as amorphous samples. In fact, due to its design, it allows to cover a range of momentum transfer wider enough to collect the structure function of amorphous samples in order to compute their radial distribution function avoiding the problems related to the mathematical procedure of data handling². Moreover, this diffractometer permits to measure the small angle scattering necessary for the study of organized microstructure³. Some recent applications were

^(c) Corresponding author: fax + 39 091 590015, E-mail: caponett@unipa.it

related to the study of the kinetics of phase transition of some materials⁴. In addition, the white beam emitted by the X-ray source and the wide range of operational power revealed to be an additional powerful tools in order to get, contemporary to the structural information, the elemental composition of samples. Generally speaking, the X-ray fluorescence involves the detection of X-rays emission due to excited electrons fluorescing within the energy levels of the atom.

Being the electron energy up to 55 keV, the tungsten (W) fluorescence L-lines of the X-ray source (W anode) as well as the fluorescence lines of the sample are simply superimposed to the diffraction patterns. A limit of the instrument is the impossibility to reveal elements up to calcium, given the high sensibility of the first channels of the detector to the instrumental noise.

The peculiar design of the instrumental components permits to place big samples in the centre of the instrument in such a way that the area to be investigated is in the optical focus. The optical focus of the instrument is the point where the detector is focused on the beam. It has to be underlined that the exact positioning of the area of the sample in the focus is a necessary step to avoid distortion on the diffraction peaks and presents the advantage to collect fluorescence data only from the scattering volume. The maximum sample size is fixed by the open space and can be as big as 15 cm wide, 50 cm long and 80 cm high. During a measure, the specimen is maintained fixed, but it is possible to move it along the three cartesian axes in such a way to get a mapping on a portion of the sample. Another peculiarity of the instrument is the possibility to make measurements either in transmission or in reflection geometry. This important feature allows obtaining information about the surface layers of a sample.

Based on the above potentiality of the EDXD, in this paper we draw attention to some applications that can be useful in the field of Cultural Heritage. In some cases, the samples under investigation are valuable items belonging to private collections; in some other cases, samples, without historical value, have been investigated and are reported as test cases. The main focus is to demonstrate that the instrument allows getting different kind of information, compositional as well as structural, in different experimental conditions, some of which cannot be obtained by using the commercial devices. Finally, in order to support the quality of the information available, the data obtained for three ancient and one modern papers were compared with those collected by using other techniques: Angle Dispersive X-ray Diffraction, Scanning Electron Microscopy, micro X-ray Fluorescence.

EXPERIMENTAL

Energy Dispersive X-ray Diffractometer

A photograph of the EDXD diffractometer is given in figure 1. The diffractometer operates in vertical θ/θ geometry and is equipped with an X-ray generator, a collimating system, two step motors, and a solid-state detector connected via an electronic chain to a multichannel analyzer. The X-ray source is a Seifert tube (W target) operating at 55 kV and 45 mA whose Bremsstrahlung radiation is used whereas the detecting system is composed of a solid state photon (HPGe) detector (Ortec) cooled by an X-cooler system and connected to a PC through ADCAM hardware. Both the X-ray source and the detector can rotate, by an angle θ , around the focus where the volume of the sample to be investigated is placed. The emitted photons are detected and counted as a function of their energy. It is worth noticing that the photon energy range available is independent from the θ/θ geometry, this implies that the fluorescence lines are insensitive to θ . On the contrary, the diffraction peaks positions depend on both the energy and θ . This implies that changing θ , the diffraction peaks move to lower or higher energies. In order to get a diffractions pattern directly comparable with that achievable by means of Angle Dispersive X-ray Diffractometer, the energy have to be transformed in transfer momentum Q

$$Q = cost * E * sin\theta \quad (1)$$

where $cost = 1.01354 \text{ \AA}^{-1} \text{ keV}^{-1}$ and E is the energy. On this basis, in order to attain a Q -range as wide as possible, being the energy range determined by the operational set-up, the data collection has to be performed at various θ angles. Concerning the diffraction data, the main disadvantage of the instrument is the uncertainty ΔQ associated to the transfer momentum that is the result of the uncertainties associated to θ ($\Delta\theta = 0.001^\circ$) and to E (0.05 keV). The zone of each sample to be analyzed has been localized by means of a fluorescent screen that allows tracing the beam. The screen has been then removed to perform the measurements.

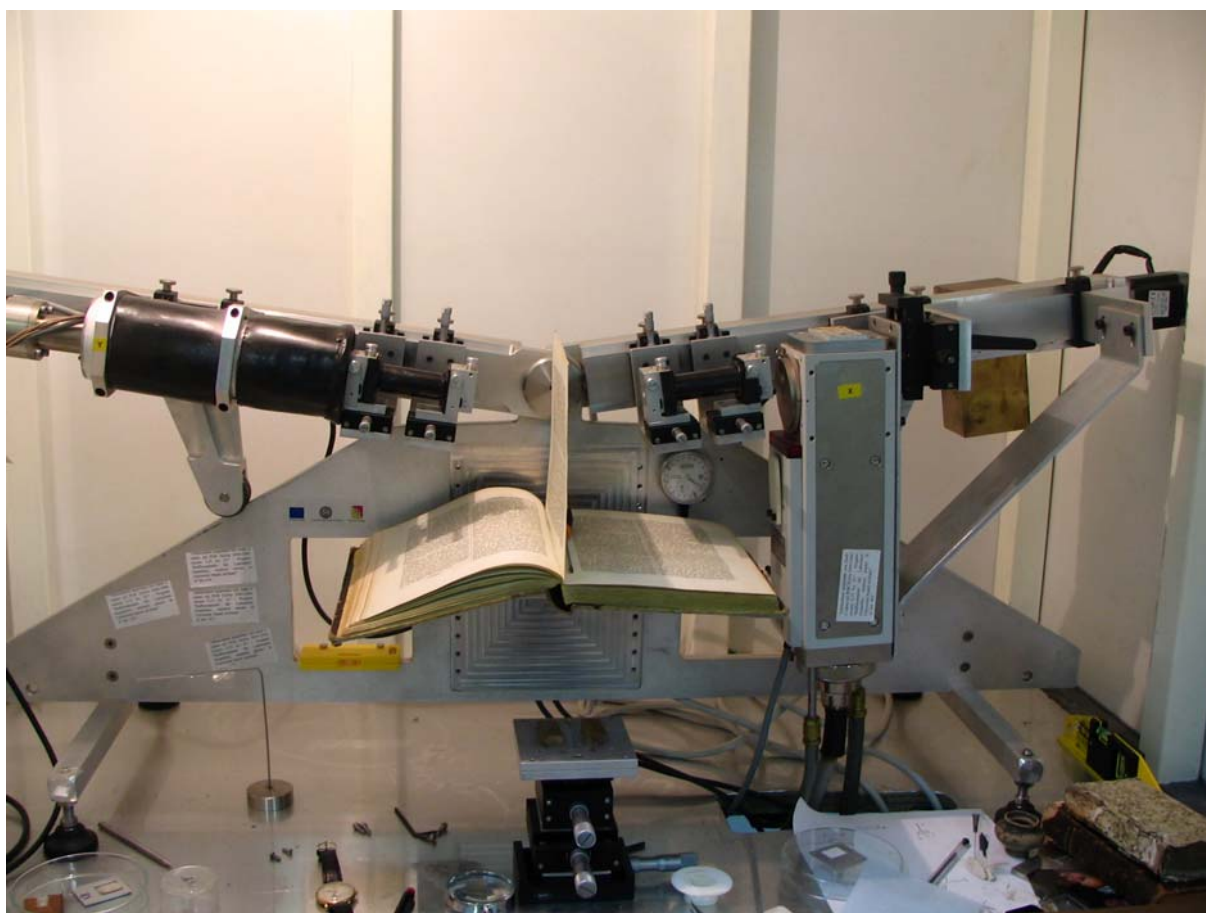


FIGURE 1. - Photograph of the Energy Dispersive X-ray Diffractometer. The investigated samples were placed in the optical centre of the instrument without any preliminary preparation or removal of fragments.

Angle Dispersive X-ray Diffractometer.

Measurements were performed by means of a Philips PW 1050/39 diffractometer in the Bragg-Brentano geometry using Ni filtered Cu K_α radiation ($\lambda = 1.54178 \text{ \AA}$). The X-ray generator worked at a power of 40 kV and 30 mA and the resolution of the instrument (divergent and antiscatter slits of 0.5°) was determined using $\alpha\text{-SiO}_2$ and $\alpha\text{-Al}_2\text{O}_3$ standards free from the effect of reduced crystallite size and lattice defects. The diffraction pattern has been reported as a function of transfer momentum:

$$Q=4\pi/\lambda*\sin\theta \quad (2)$$

Scanning Electron Microscopy. SEM analysis has been performed by using a Philips XL30 equipped with a Energy Dispersive X-ray device. Samples were supported on the stubs by carbon paint and coated with gold. The accelerating voltage was tunable between 20 and 30 kV for SEM measurement, while for micro XRF was 25 kV.

RESULTS AND DISCUSSION

The goal of the work is to elucidate the potentiality of the instrumentation in the field of Cultural Heritage. Hence, the examples here reported are classified on the basis of the information that can be achieved rather than on the basis of sample kind.

In the first of the following three sections, the simultaneous detection of: - fluorescence and the amorphous contribute, - fluorescence and diffraction of a simple crystalline sample and, - fluorescence and diffraction of a more complicated crystalline sample will be discussed.

In the second one, the possibility to obtain informations on samples covered by layers of various materials will be presented.

In the last section, a more exhaustive study on paper samples will be reported.

1. SIMULTANEOUS DETECTION OF DIFFRACTION AND FLUORESCENCE

1.i - EDXD spectrum collected at $\theta = 4.3^\circ$ for a developed film is shown in figure 2. The spectrum extends up to 50 keV due to the operational conditions, i.e. 50 kV and 40 mA. The same operational conditions apply to all the samples here reported, hence these will not be specified any more.

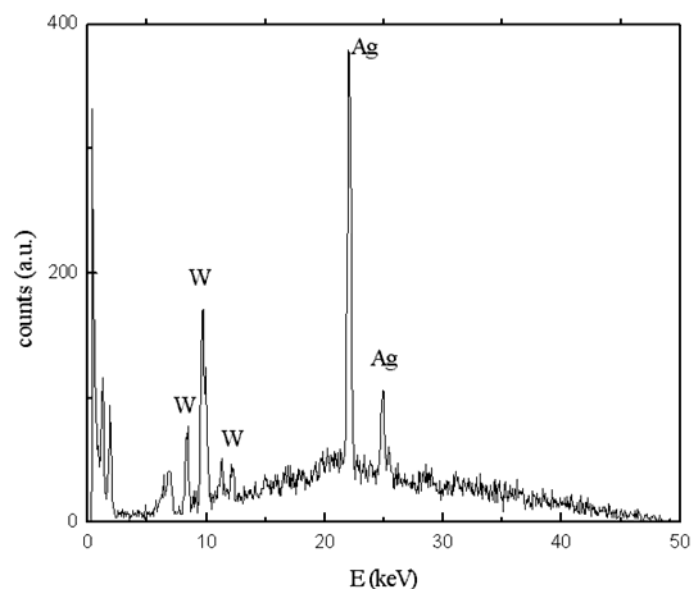


FIGURE 2. - EDXD spectrum for the developed film.

In addition to the fluorescence lines of the tungsten, the ones of silver were identified. The non flat contribution to the spectrum has to be attributed to features characteristic of the amorphous polyethylene terephthalate material, whose structure, i.e. radial distribution function, if required, can be resolved by means of a certain number of measures covering a wide Q -range. Since the purpose of the present work, this aspect has not been deepened.

1.ii - EDXD spectra have been collected at $\theta = 9.2^\circ$ on a ring composed by alloys of two different colours, yellow and white, interconnected. Two photographs of the ring and the spectra of the two portions, shown as a function of energy, are reported in figure 3.

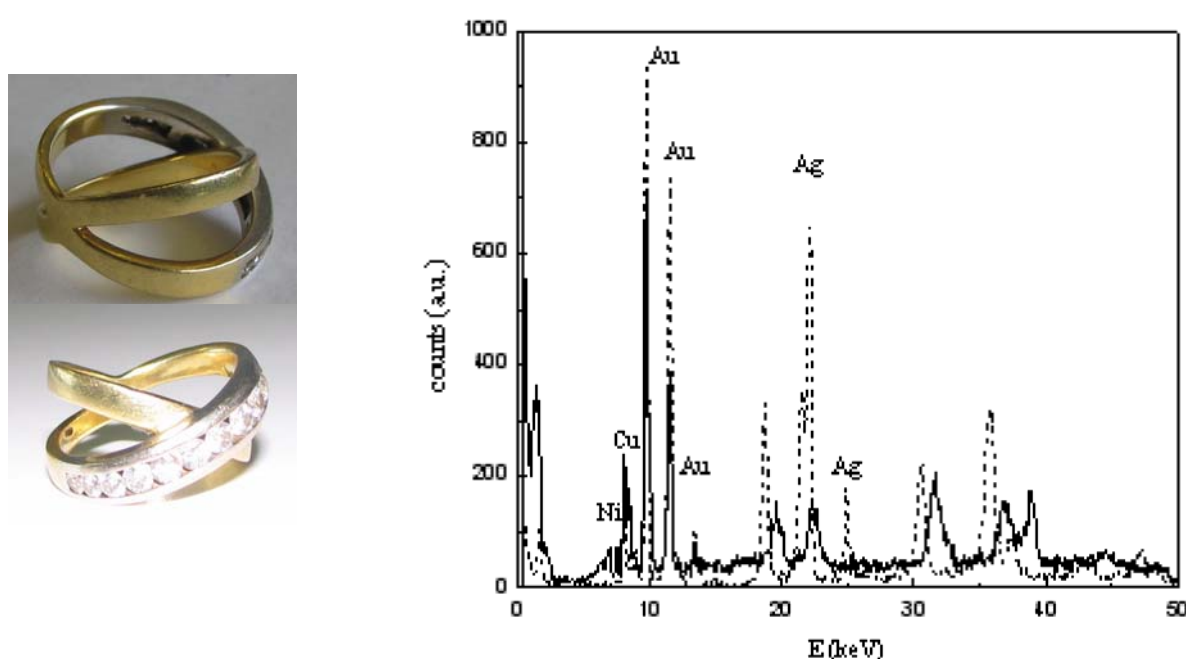


FIGURE 3. - Photographs of the ring in which the two portions at different colours are evident and EDXD spectra obtained for the white alloy, continuous line; and the yellow alloy, dashed line.

In the spectra, the fluorescence lines of the elements composing the alloys are evidenced. All other contributions are diffraction peaks due to the crystalline structure of each sample.

The yellow metal results composed by gold, silver and copper, i.e. the common composition of gold alloy used in jewellery⁵. The white alloy is composed by gold, copper and nickel, while it does not contain neither palladium, usually added to precious white gold alloys, or zinc. In order to achieve quantitative data on the relative amounts of the components, a calibration line is necessary, as in the standard XRF analysis.

In order to determine easily the crystalline structure of the sample, the energy scale was converted in momentum transfer scale by applying equation 1; the resulting spectra are displayed in figure 4. Spectra have been truncated for the contribution at energies lower than 13 keV because in the 0 – 13 keV range ($0 - 2 \text{ \AA}^{-1}$) only the fluorescence lines are present.

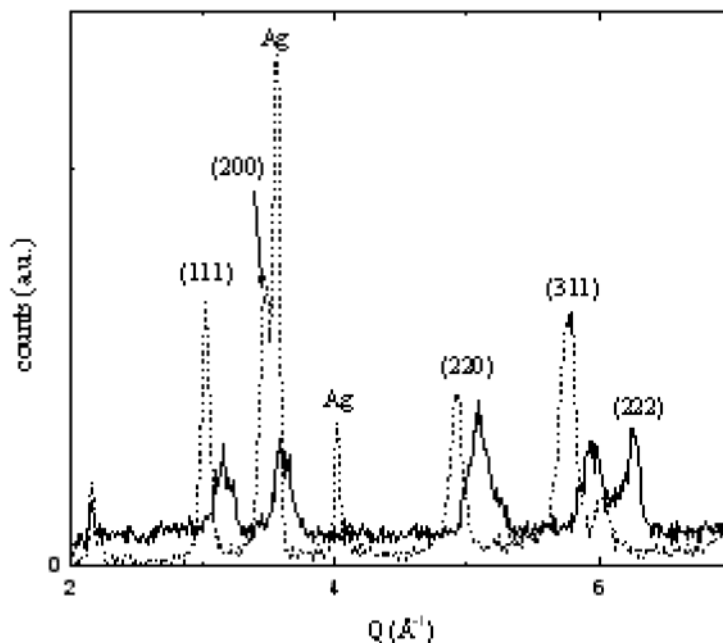


FIGURE 4. - EDXD data of the ring: white alloy, continuous line; yellow alloy, dashed line.

Clearly, the crystalline structure of the two alloys is different. The labelled peaks are the reflections arising from the cubic centred face (cfc) space lattice common to gold, silver and copper, components of the yellow alloy. The presence of nickel in the white alloy causes a distortion of the cfc lattice as evidenced from the disappearing of the higher order (222) reflection and from the displacement at higher Q -values of the others reflections. Moreover, these measurements illustrate how it is possible to acquire data on various part of the same item. This allows to obtain mean compositional information on big portion of a sample while, as known, fluorescence mapping performed by using micro XRF coupled with scanning or transmission electron microscopy, allows to obtain the punctual composition on a small sample or a small portion of a specimen.

1.iii – EDXD spectra collected for an ancient coin, together with its photograph, are shown in figure 5. Data have been acquired at three different values of θ (6.7, 8.9 and 11.3°) in order to discriminate the fluorescence from the diffraction contribution in the spectrum that display a large number of peaks. The coin belongs to a private collection and its provenance as well as its age is doubtful. It appears to be damaged and covered by a layer of oxide. The fluorescence lines of the elements composing the coin are labelled and are superimposed to the diffraction pattern. They can be discriminated from the diffraction peaks by looking at the graph where counts are reported vs. energy, figure 5A. For clarity reasons, spectra at 8.9 and 11.3°, have been added by a constant amount. It appears that some peaks are insensitive to the change in θ , these are ascribable to the fluorescence energy while those moving to lower energies by increasing θ can be identified as diffraction peaks. Once the energy is converted, by means of equation 1, in transfer momentum, the diffraction peaks related to a particular reflection fall to the same Q -value, as can be inferred from figure 5B. Spectra have been truncated for the contribution at energies lower than 10 keV because

in the 0 – 10 keV range ($0 - 1.2 \text{ \AA}^{-1}$ at $\theta = 6.7^\circ$; $0 - 1.6 \text{ \AA}^{-1}$ at $\theta = 8.9^\circ$ and $0 - 2.0 \text{ \AA}^{-1}$ at $\theta = 11.3^\circ$) only the fluorescence lines are present. In the same graph, the fluorescence lines are labelled by * and move to higher Q -values on increasing θ . It is worth noticing that, on increasing θ , both the minimum and the maximum Q -value increase too. This, as explained in the experimental section, is a direct consequence of Q dependence from E and θ .

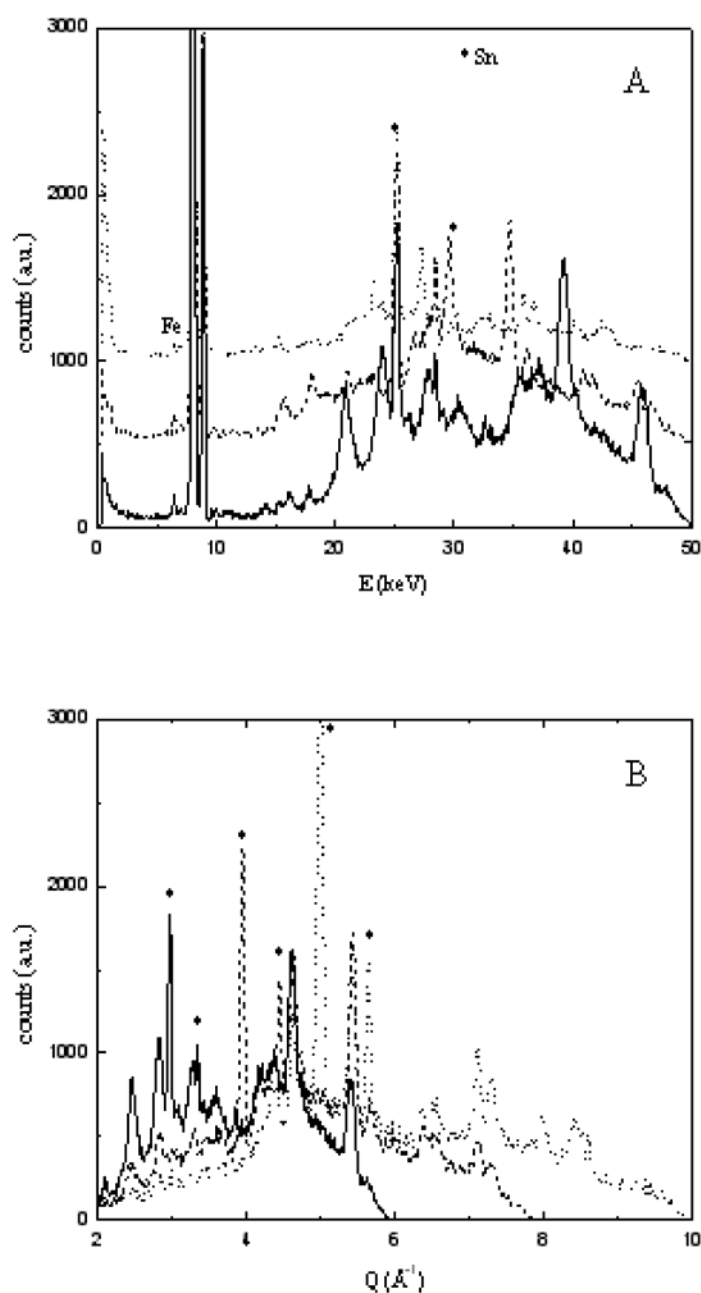


FIGURE 5. - Ancient coin photograph and EDXD spectra collected at: 6.7° , continuous line; 8.9° , dashed line, and 11.3° , dotted line, respectively. A: counts vs. E , B: counts vs. Q .

In addition to the fluorescence lines of the tungsten, the strongest ones, those of iron and tin were identified. All other contributes to the spectra are the diffraction peaks. Some of the peaks can be attributed to the cubic and to the hexagonal phases of the 3:1 FeSn alloy. Given the very large number of crystallographic structures that iron and tin can generate at various compositions, for a complete attribution of all peaks the stoichiometry of the alloy must be known.

2. BURIED SAMPLE

In order to exploit the applicability of the technique to samples that for particular reasons are maintained inside a preserving environment, measurements on a coin buried in a block of polymethylmethacrylate (PMMA), on the hand under the glass of a clock and on layered samples like a photos, have been performed.

2.i – A buried coin whose photographs in two different views are reported in figure 6, has been investigated. The thickness of the polymeric coverage is c.a. 2 mm and 1 mm on the two faces. EDXD spectra collected from the face covered by 1 mm of PMMA are reported in figure 6. In order to clarify the way in which the sample has been moved, a scheme of the measurements is reported in the same figure.

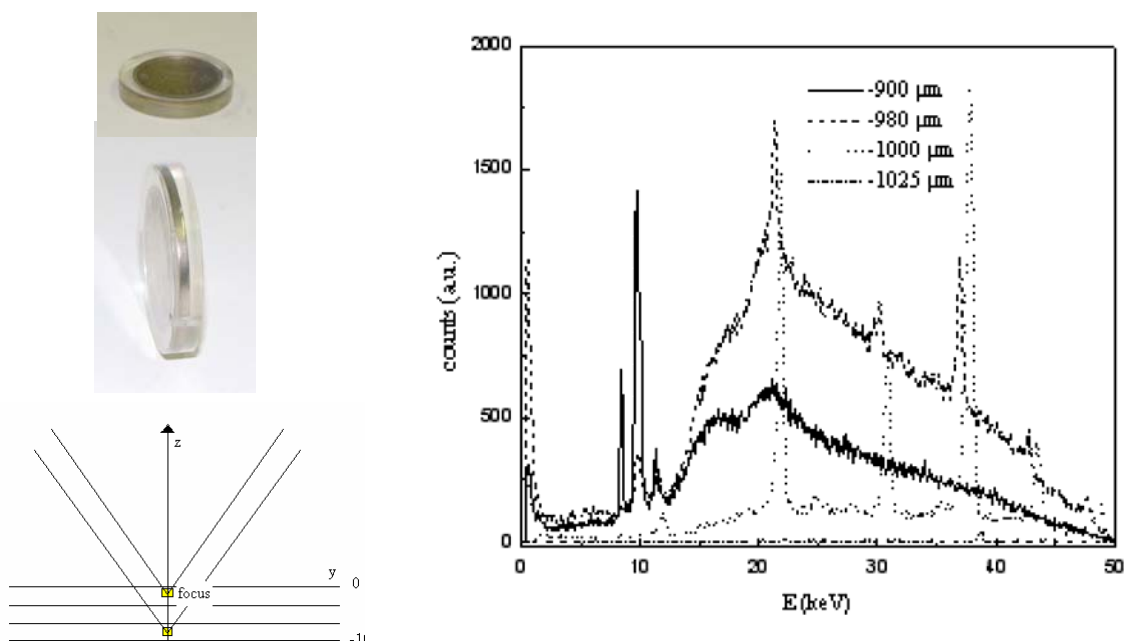


FIGURE 6. - Top and side view of the coin buried in the PPMA block, measurement scheme and EDXD spectra collected at various z-position of the sample.

The coin placed on the xy-plane, have been moved along z up to when the beam incides on the surface in the optical axis of the instrument. This position, called the z-zero position, has been recognized as the point where photons, coming from the surface, start to be detected. Starting from this point, data have been collected moving step by step (20 μm) the sample along z. Up to a

distance of - 940 μm from the surface, only the spectrum characteristic of the amorphous PMMA⁶ is revealed. Once the polymer/coin interface is reached, the diffraction lines of the coin appear superimposed to the amorphous spectrum. These lines become very intense at - 1000 μm distance from the surface. Moving below the polymer/coin interface any signal can be revealed. This is a consequence of the position of the focal point that in these condition is below the interface, at a depth higher than the mean free path, so avoiding the X-ray to exit.

2.ii – With the purpose to acquire information on one hand of a clock without removing the glass coverage, EDXD spectra have been collected at various z-position, following the scheme shown in figure 6, and are reported in figure 7, together with a photograph of the clock.

The first spectrum was collected on the glass, the fluorescence lines of the source and the amorphous glass contribute to the scattering are both present (dashed line in figure 7). On moving the sample along z-axis for - 50 μm (dot-dashed line), the spectrum is similar to the first one, but the features becomes less intense due to the absorption of the X-ray by the material. At z-position higher than - 2000 μm , the spectrum is flat. The features ascribable to the hand appear at a distances of - 5050 μm (continuous line).

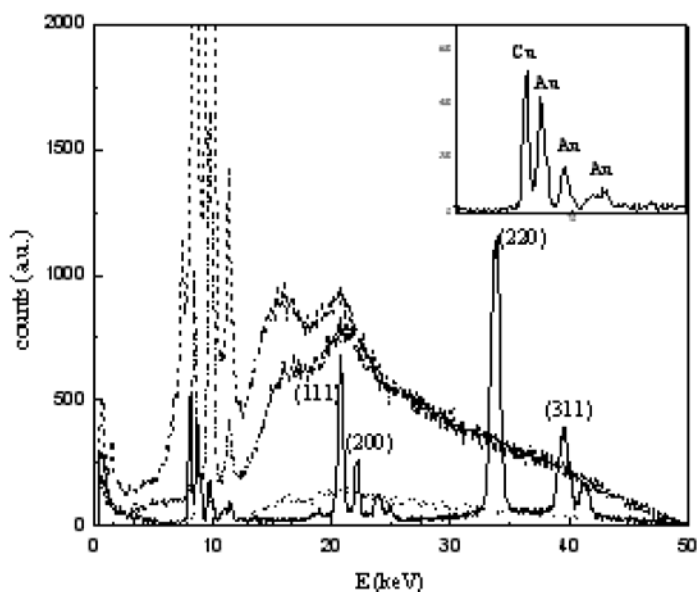


FIGURE 7. - Top side view of the clock and EDXD spectra collected at various z-position of the sample: glass, dashed line and dot-dashed lines; air under glass, dotted line; hand, continuous line, respectively. In the inset, the enlargement of the hand spectrum in the energy range 5 – 15 keV is reported.

In the spectrum, the fluorescence lines of copper and gold as well as the diffraction peaks of the (cfc) alloy have been identified.

2.iii - It is well known that, depending on the energy and the radiation incidence angle as well as on the elemental composition of the sample, X-ray beam mean penetration depth is different. Since the photons detected are only those generated in the focus of the instrument, informations from

different layered zone of the same sample can be obtained in a non destructive way, i.e. without removing any layer from a surface.

EDXD spectra were collected from various old photos belonging to a private collection (Saladino's family). These photos have been printed in Milan, as inferred from the logo in the back of photos. Photos have been placed on the xy-plane, then have been moved along z up to when the beam incides on the surface in the optical axis of the instrument. From the zero position, recognized following the procedure explained in the section 1.i, the samples have been moved, step by step (5 μm), along z-axis up to -125 μm following the same scheme reported in figure 6. From the experimental results, the photos can be grouped in two classes whose peculiarity are highlighted by the two samples here reported. The two photos have been labelled as Chinese and Priests based on the scenario. A picture of them is reported in figure 8 together with some representative EDXD spectra, collected at different depths.

From spectra inspection of Chinese photo, it emerges that silver is present on the surface, where no diffraction pattern is observed. Changing the sample height, the disappearing of silver fluorescence line could be assumed as an indication of the thickness of the surface layer, that spread for 75 ± 10 μm . The same deduction can be drawn for the Priests photo, in which the silver layer spread for 50 ± 10 μm .

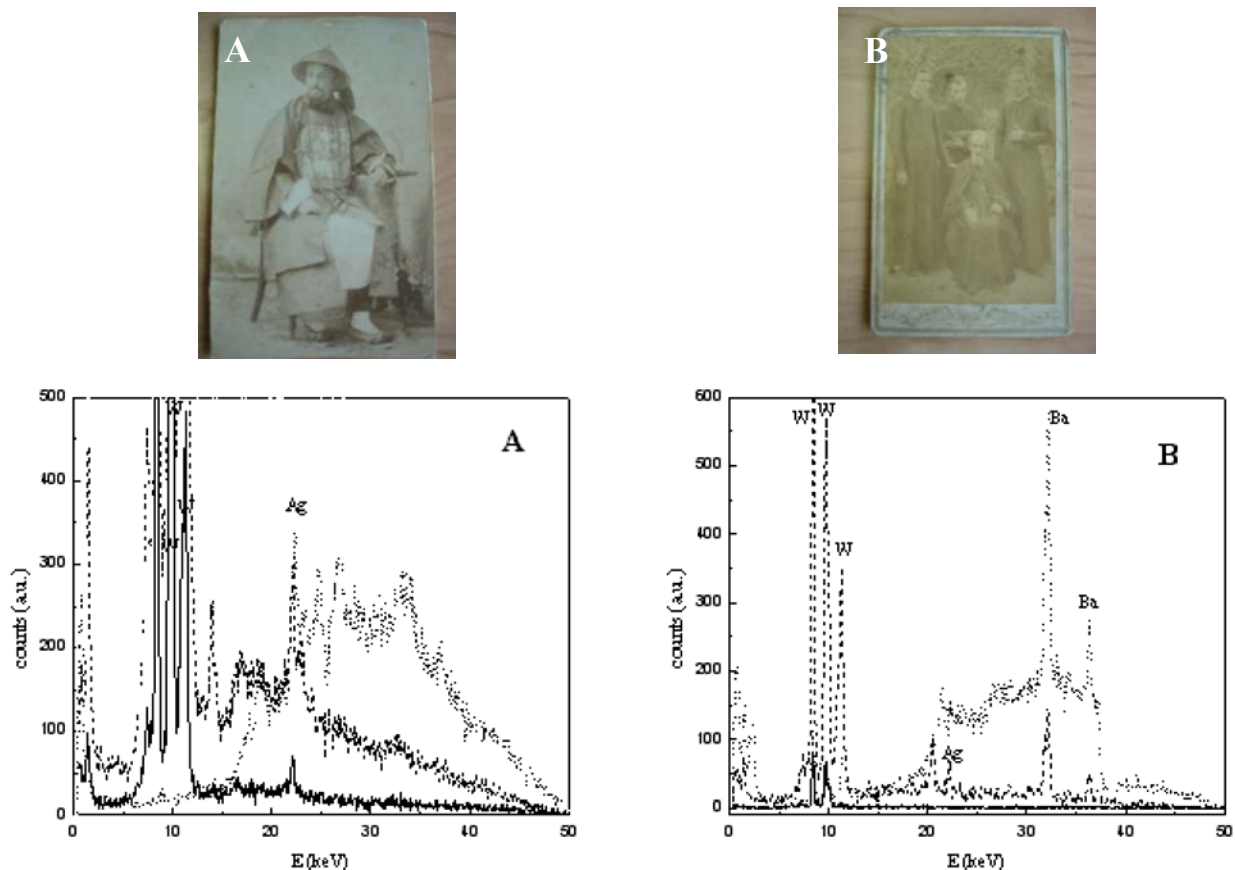


FIGURE 8. - Chinese (A) and Priests (B) photos and some representative EDXD spectra collected for each of them. In both graphs the z-values are: 0, continuous line, -25, dashed line and -125 μm , dotted line.

Moreover, on increasing the depth of the inspected volume, in both spectra the diffraction features of the cardboard appear. In addition, for the Priests photo the presence of barium fluorescence peaks, whose intensity increases with depth, proves the presence of this element in the support cardboard. In order to support these findings, measurements have been repeated on the back of the two photos. Results are shown in figure 9.

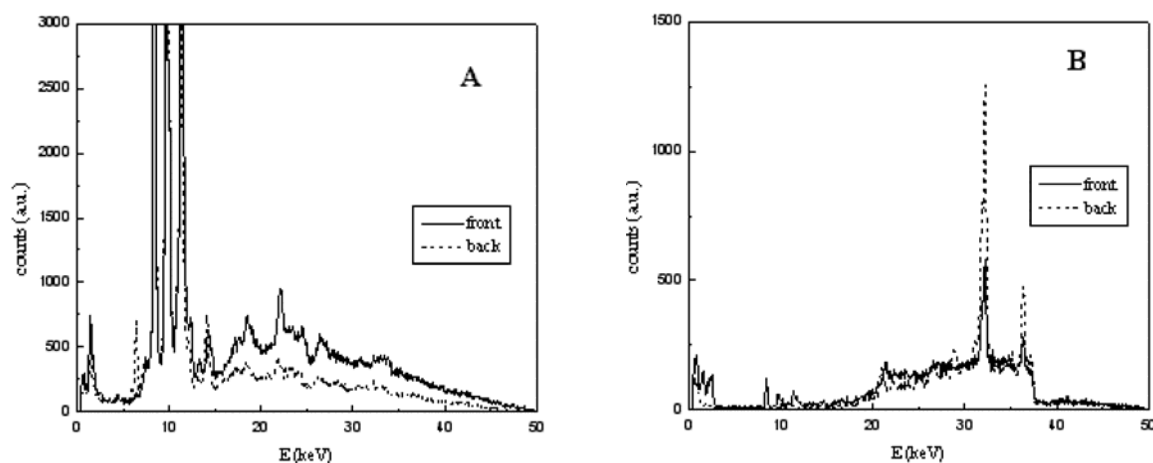


FIGURE 9. - EDXD spectra collected, in the same geometrical configuration, for front and back side of China and Priest photos.

The comparison of spectra collected from front and back side indicates that the presence of Ba and the detected structure are the ones of the cardboard.

The findings from the three samples examined support the feasibility of the investigation on a layered sample making possible to “see” the inner part of the sample as if the outer part was removed.

3. DETAILED INFORMATION

Another interesting feature of the instrument is the possibility to perform measurements on any portion of a page of a book without disassembling it. EDXD measurements have been performed on four samples, a 1672 book identified as “seicentina”, a 1870 book identified as “messale”, a non dated booklet whose provenance is from the Iranian region identified as “iranian”, and a 2004 white paper commercially available identified as “modern paper”. Photographs of the samples are reported in figure 10.



FIGURE 10. - From left to right, photographs of seicentina, messale and Iranian books.

Measurements have been performed on:

- the edge of a page of the :A) seicentina, B) messale and C) Iranian, that, besides to be no written, have been selected for the absence of spots or other damages. These zones appeared clean, clear and in fairly good conditions;
- the edge of a page of the seicentina (D sample) with extended dark shadow without any other apparent kind of damages;
- black (E sample) and red (F sample) ink areas, that not appeared damaged, for the Iranian booklet;
- a portion of a sheet of the “modern paper” (G sample).

Data have been collected at $\theta = 4.5^\circ$ on the A, B, C and G samples and spectra are shown in figure 11 as a function of the transfer momentum Q . The Q -scale extend from 1 up to 4 \AA^{-1} , the contributions due to energies lower than 12.6 keV have been truncated because contain only the fluorescence peaks as will be discussed later.

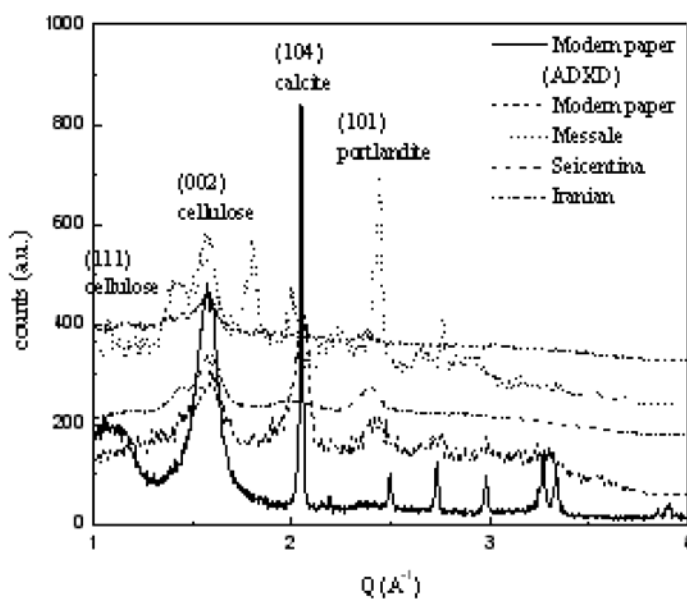


FIGURE 11. - EDXD spectra, reported as counts vs. transfer momentum, of seicentina, messale, Iranian edge of page and modern paper. For comparison, the ADXD diffractogram, collected for the modern paper is reported.

In the same figure the conventional (ADX) pattern (continuous line) collected only for the modern paper is also reported. The same measurement has not performed on the other samples because this implies the removal of important fragments of the books.

All the EDXD scans as well as the ADXD pattern, contain the characteristic peaks of crystalline form of cellulose. In particular, a strong peak centered at $Q = 1.6 \text{ \AA}^{-1}$ corresponding to the (002) reflection of cellulose is evident in all the patterns while a less pronounced peak, at $Q \sim 1 \text{ \AA}^{-1}$, corresponding to the (111) reflection is clearly evident only for the modern paper. These peaks result less pronounced for the Iranian sample.

The broad diffraction peak, positioned at $Q \sim 2.1 \text{ \AA}^{-1}$, is common to the modern, the seicentina and the Iranian sample and it is not present in the *messale* paper. It can be attributed to the (104) peak of calcite, i.e. calcium carbonate, whose presence is usually explained as the result of the reaction between the calcium hydroxide retained in the paper and the atmospheric carbon dioxide. This interpretation is also enforced from the presence of the diffraction peak centered at $Q \sim 2.4 \text{ \AA}^{-1}$ which is due to a residual calcium hydroxide preserved in the crystalline form of portlandite (101 reflection). Incidentally, the strong peaks centred at $Q \sim 2.4$ and 2.8 \AA^{-1} in the *messale* sheet, have to be attributed to the $K_{\alpha 1}$ and $K_{\alpha 2}$ fluorescence lines of barium. Calcium carbonate, sometimes with a mixture of calcium hydroxide, can be detected in old papers made in accordance with the Italian method⁷. In addition, the peak of calcite in the modern paper is very narrow and much stronger than that detected in old one. This finding suggests that the calcium percentage in the modern paper is much higher with respect to older ones. A possible explanation of this observation is that different papermaking technologies directly result in different structural features of the paper itself. It is worth noticing that fast EDXD measurements can easily detect such inner structural differences.

The evident differences in the relative intensities of diffraction peaks are, probably, due to different structural arrangements at a nanometric level. In order to support this hypothesis some scanning electron micrographs have been collected on the four samples.

Micrographs, shown in figure 12, indicate that the texture of specimens is perfectly in line with the findings of EDXD. In fact, fibres appear to be well preserved for the seicentina as well as for the Iranian and modern paper, while the fibres of the *messale* are less distinct. In addition, the modern paper presents calcite particulate between fibres whose size and amount is appreciably higher compared to the other samples.

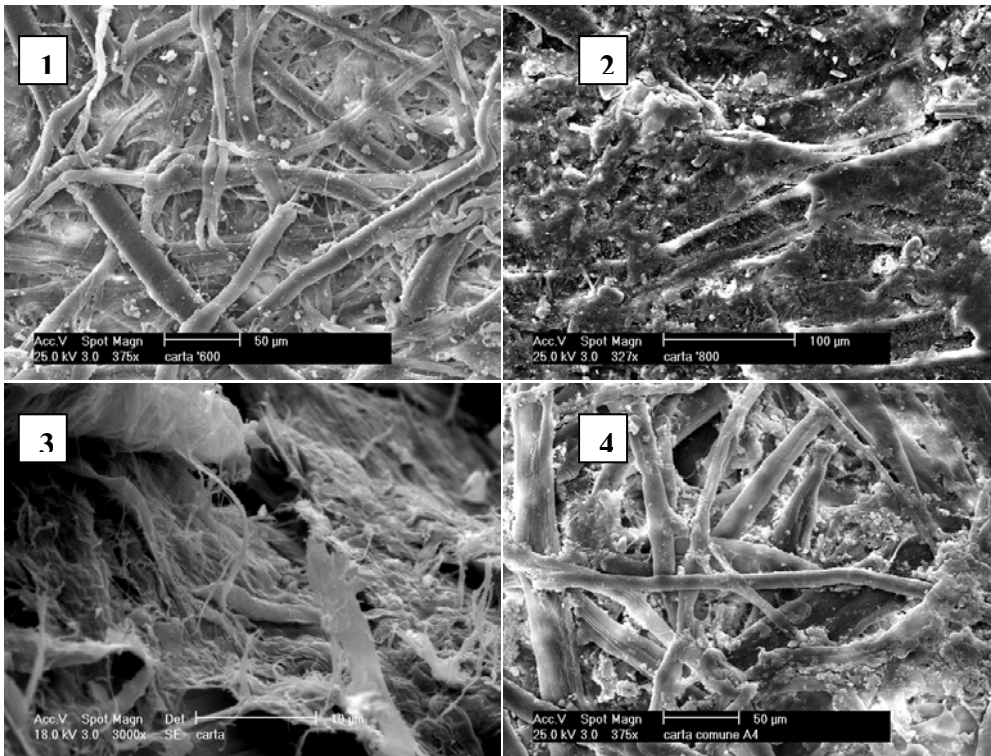


FIGURE 12. - SEM Micrographs of: 1) seicentina, 2) messale, 3) Iranian and 4) modern paper.

Indeed, paper samples are expected to give distinct XRD patterns as a function of the state of deterioration. Systematic EDXD analyses could reveal alterations in the structural organization of cellulose due to factors such as fire, humidity or pollution levels. In order to deepen such aspect, EDXD measurement has been performed on the D) sample, i.e. the brown edge of a seicentina page. Data collected and handled as previously explained, are reported in figure 13, where for comparison the spectrum collected for the A) sample, i.e. the clear edge of the seicentina page, is also reported.

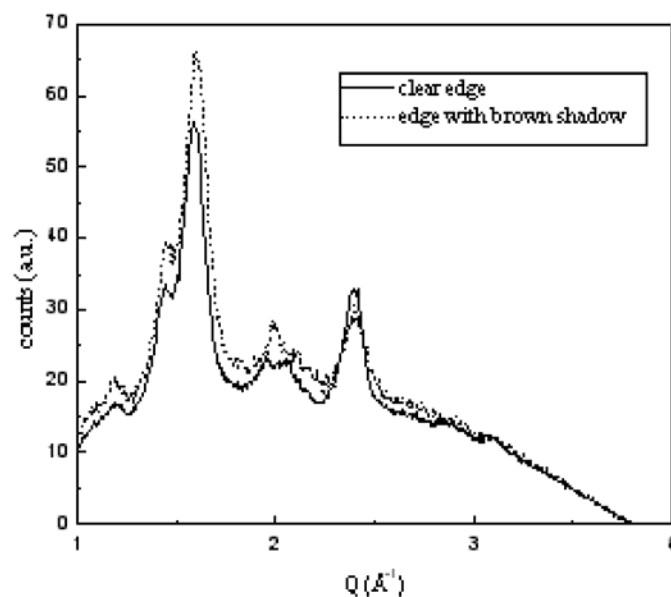


FIGURE 13. - Comparison of EDXD diffractogram of different part of seicentina.

The almost complete coincidence of the two signals suggests that the brown appearance of the paper cannot be attributed to a real degradation process. On the other hand, the extension and the shape of this region suggest that the book has been soaked with water and/or some other liquid during its long history.

In order to get light on the composition of the samples, in figure 14 the EDXD portion, up to 15 keV, of the full patterns of the same samples are reported.

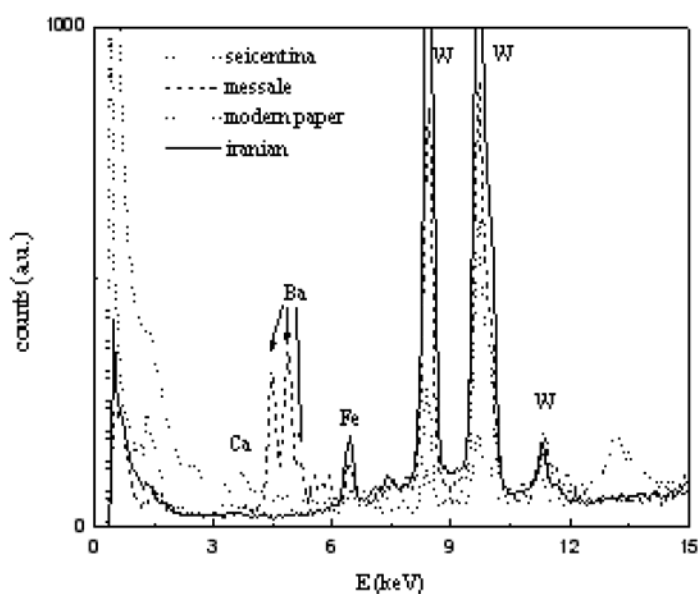


FIGURE 14. - EDXD spectra of seicentina, messale and Iranian clear edge of the page and for “modern paper”.

In all the investigated samples traces of Fe are evident. Interestingly, modern paper shows a very low percentage of Fe with respect to older paper and a higher Ca content in agreement to the discussed features of the diffraction pattern of figure 11 and the messale display the presence of barium rather than calcium. Again, these compositional differences are directly interpretable in terms of the different papermaking technologies⁷. In order to support these findings, micro XRF spectra have been collected and reported in figure 15.

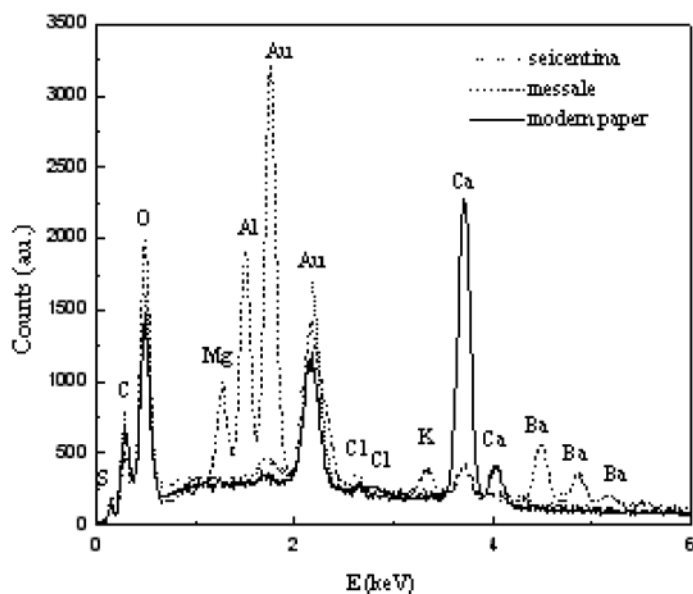


FIGURE 15. - Micro XRF patterns of “seicentina”, “messale” and “modern paper”.

Beside the presence of light elements like sulfur, carbon, magnesium, aluminum, chlorine and potassium, results are perfectly in line with those reported in figure 14.

Finally, the comparison of spectra collected for E and F samples, i.e. the black and red ink areas of the Iranian book, reported in figure 16, indicate the presence of mercury in the red ink.

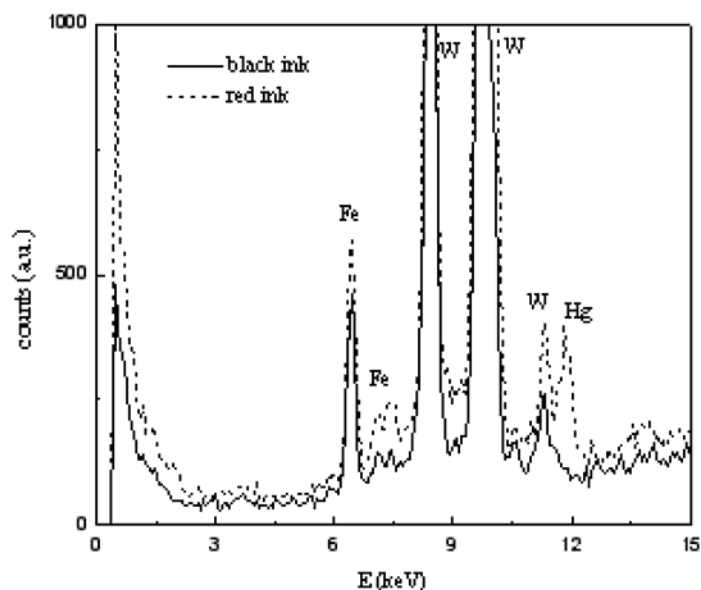


FIGURE 16. - EDXD spectra of Iranian black and red ink areas.

CONCLUSIONS

A new Energy Dispersive X-ray Diffractometer was used to collect data from various items, assumed as test case for things in the field of Cultural Heritage.

It is worth remembering that, with respect to traditional diffractive techniques, EDXD presents several advantages: (a) the source emits an intense white beam that allows collecting the entire spectrum simultaneously; (b) measurements are not dependent from the intensity fluctuation of the primary beam; (c) the time of measurements is often strongly reduced with respect to traditional angular dispersive techniques and (d) any part of the diffractometer moves during data acquisition, therefore, the errors due to misalignment are reduced. The instrument reveals to be well suited in order to get both compositional and structural information from a unique measurement. Even if the resolution of the instrument is lower than that of commercial devices, both compositional and structural data result in a very good agreement with those collected with other techniques: Angle Dispersive X-ray Diffraction, Scanning Electron Microscopy, micro X-ray Fluorescence.

The design of the instrument results particularly advantageous in the field of Cultural Heritage. In fact, it allows obtaining data from a very large variety of samples without any particular preparation and without collection of any portion. Moreover, the possibility of collecting data in transmission as well as in reflection mode, makes possible to investigate samples having peculiar geometries. The reflection mode allows to collect data on bulk samples. It can be successfully used to get information on layered samples and, eventually, to measure the thickness of a layer. Finally, it allows to collect data from a buried samples; this application can be successfully employed to investigate samples having coverage extending from few microns up to some millimetres depending on the composition in terms of percentage of low atomic number atoms.

Some of the above experiments cannot be performed by using the commercial devices.

Acknowledgements - Thanks are due to the Università di Palermo for financial founding. We are deeply indebted with Dr. Antonino De Maria, Mr. Vincenzo Saladino and Mr. Alberto Urso for gently providing us some of the investigated samples and with Dr. Paolo Guerra for performing SEM microscopy.

REFERENCES

- 1) R. Caminiti, V. Rossi Albertini, *Int. Rev. Phys. Chem.*, **18**, 263 (1999)
- 2) M. Di Marco, M. Port, P. Couvreur, C. Dubernet, P. Ballirano, C. Sadun, *J. Am. Chem. Soc.*, **128**, 10054 (2006)
- 3) G. Caracciolo, G. Mancini, C. Bombelli, R. Caminiti, *Chem. Phys. Lett.*, **386**, 76 (2004)
- 4) R. Caminiti, G. Caracciolo, M. Pisani, P. Bruni, *Chem. Phys. Lett.*, **409**, 331 (2005)
- 5) W.S. Rapson, *Gold Bull.*, **23**, 125 (1990)
- 6) B. M. Ginzburg, A. S. Smirnov, S. K. Filatov, L. A. Shibaev, E. Yu. Melenevskaya, A. V. Novoselova, and A. A. Shepelevskii, *Russian Journal of Applied Chemistry*, **76**, 457 (2003)
- 7) J. Dąbrowsky, J. S. G. Simmons, *FIBRES & TEXTILES in Eastern Europe*, **11**, 8 (2003)